THE JOURNAL OF PHYSICAL CHEMISTRY B

Article

pubs.acs.org/JPCB

Ion Pair Reinforced Semi-Interpenetrating Polymer Network for Direct Methanol Fuel Cell Applications

Chunliu Fang,[†,‡] David Julius,[‡] Siok Wei Tay,[§] Liang Hong,*[,‡,§] and Jim Yang Lee*[,†,‡]

[†]National University of Singapore Graduate School for Integrative Science and Engineering, 28 Medical Drive, 117456, Singapore
[‡]Department of Chemical and Biomolecular Engineering, National University of Singapore, 4 Engineering Drive 4, 117576, Singapore
[§]Institute of Materials Research and Engineering, A* STAR, 3, Research Link, 117602, Singapore

Supporting Information

ABSTRACT: This paper describes the synthesis of ion-pair-reinforced semi-interpenetrating polymer networks (SIPNs) as proton exchange membranes (PEMs) for the direct methanol fuel cells (DMFCs). Specifically, sulfonated poly(2,6-dimethyl-1,4-phenylene oxide) (SPPO), a linear polymer proton source, was immobilized in a brominated PPO (BPPO) network covalently cross-linked by ethylenediamine (EDA). The immobilization of SPPO in the SIPN network was accomplished not only by the usual means of mechanical interlocking but also by ion pair formation between the sulfonic acid groups of SPPO and the amine moieties formed during the cross-linking reaction of BPPO with EDA. Through the ion pair interactions, the immobilization of SPPO polymer in the BPPO network was made more effective, resulting in a greater uniformity of sulfonic acid cluster distribution in the membrane. The hydrophilic amine-containing cross-links also compensated for some of the decrease in proton conductivity caused by ion pair formation. The SIPN membranes prepared as such showed good proton conductivity, low methanol permeability, good mechanical properties, and dimensional stability. Consequently, the PPO based SIPN membranes were able to deliver a higher maximum power density than Nafion, demonstrating the potential of the SIPN structure for PEM designs.

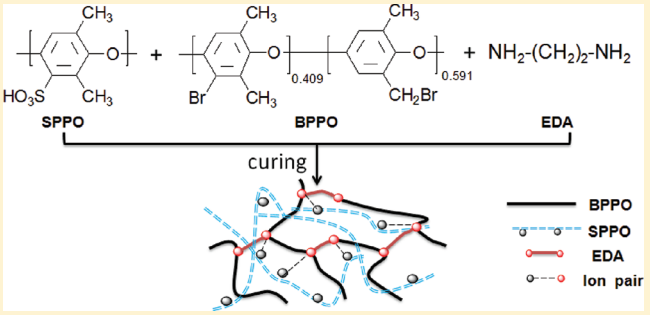

1. INTRODUCTION

As a key component of the direct methanol fuel cells (DMFCs), the proton exchange membrane (PEM) must concurrently satisfy several functional requirements such as high proton conductivity, low methanol permeability, and good mechanical stability. However, there is a trade-off between proton conductivity and mechanical properties in most PEM designs—while proton conductivity desires strong hydrophilicity, the latter also introduces excessive swelling to undermine the membrane integrity.[1] There are a few approaches to improve the membrane mechanical properties. Among them, ionic cross-linking and covalent cross-linking are the most common.[2−6] The former is better at maintaining membrane flexibility, while the latter is more hydrolytically stable.[7] However, they are not without disadvantages—ionic cross-linking lacks mechanical robustness, and covalent cross-linking often gives rise to brittleness of the membrane in the dry state.[8] PEMs containing a mixture of ionic and covalent cross-linking were therefore proposed.[9,10] Although the mechanical stability of ionically cross-linked membranes can be improved by covalent cross-linking, a marked decrease in proton conductivity is often observed because of the maldistribution of ionic cluster caused by the lack of controlled cross-linking.

A semi-interpenetrating polymer network (SIPN) is a special class of polymer composites where one or more linear (or branched) polymers percolate molecularly into a network of other polymers. It therefore provides a high degree of homogenization of the constituent polymers beneficial for the fabrication of PEMs for DMFCs. In principle, a linear ionomer can be used as the proton source to infiltrate a cross-linked network which provides the mechanical properties. The interlocked polymer structure can lead to good mixing of hydrophilic and hydrophobic phases to support a more distributed presence and connectedness of ionic clusters.[11,12] Compared with typical polymer cross-linking, the SIPN-enabled interlocked membrane matrix and morphology homogeneity are better poised to mitigate the trade-off between proton conductivity and membrane mechanical strength.

Despite the promising prospects, SIPN membranes for DMFC applications have yet to be satisfactorily demonstrated.[13−15] In many of the studies, the network polymer was cross-linked by ester linkages between carboxyl and hydroxyl groups. The hydrolysis of ester linkages under acidic and basic

Received: August 23, 2011
Revised: April 25, 2012
Published: May 17, 2012

dx.doi.org/10.1021/jp2081353 | J. Phys. Chem. B 2012, 116, 6416−6424

conditions imposes certain environmental sensitivity that can compromise the actual performance of these SIPNs.

This study proposes a new SIPN design where ion pairs are used to reinforce the SIPN structure. In typical SIPNs where the constituents are only held down mechanically, there is a strong tendency for the more mobile polymer to retreat or even withdraw from the network polymer under certain conditions or with time, resulting in phase separation and the degradation of application performance.[16−18] A solution to this problem is proposed in this study which uses ion pair formation between the linear polymer and the network polymer to strengthen their attachment. Through the ion pair interactions, the immobilization of linear polymer in the network can be made more uniform to yield stronger mechanical properties and dimensional stability. In addition, the ion pair interactions are also complemented by covalent cross-linking to increase the membrane hydrolytic stability. The SIPN was synthesized from linear sulfonated poly(2,6-dimethyl-1,4-phenylene oxide) (SPPO), brominated PPO (BPPO), and ethylenediamine (EDA) cross-linker by a one-pot thermal cross-linking procedure. PPO was chosen because it is a thermally and mechanically stable aromatic polymer with good chemical resistance. Its ease of processability and sulfonation are particularly suited for PEM fabrications.[19] Ion pairs were formed after cross-linking and strengthened the attachment of SPPO to the BPPO/EDA network. The SIPNs prepared as such contain more chemically resistant linkages to withstand the DMFC operation. Measurements of membrane dimensional changes and hydrolytic stability confirmed the improvements made to the PPO membranes for fuel cell applications.

2. EXPERIMENTAL SECTION

2.1. Materials. PPO (M_w = 30 000, T_g = 211 °C), chlorosulfonic acid (99.0−99.4%), *N*-methyl-2-pyrrolidone (NMP, 99%), and EDA were purchased from Sigma-Aldrich. BPPO (59.1% benzyl bromide and 40.9% aryl bromide as analyzed by ^{1}H NMR spectrometry) was obtained from Tianwei Membrane Corporation Ltd. of Shandong (People's Republic of China). Chloroform (99%) and methanol (99.8%) were supplied by Merck. Nafion 117 films were provided by Sigma-Aldrich.

2.2. Preparation of SPPO/BPPO/EDA SIPN Membranes. SPPO was synthesized by a published procedure using chlorosulfonic acid as the sulfonation reagent.[20] Specifically, 3.5 mL of chlorosulfonic acid was added to a PPO solution in chloroform (5 g of PPO per 100 mL of chloroform) at room temperature over a period of 30 min under vigorous stirring. The reaction was allowed to continue for 30 more minutes after the addition. The precipitate from the reaction was filtered off and dissolved in NMP and dried in an oven at 80 °C for solvent removal. The oven-dried solid was washed with deionized water until the rinsewater was pH 6−7 and then vacuum-dried. The ion exchange capacity (IEC) of the SPPO synthesized as such was determined to be 2.58 mmol g^{-1}, or 39.1% degree of sulfonation according to the relation given in the literature.[21] BPPO and the synthesized SPPO were separately dissolved in NMP to a concentration of 30 mg mL^{-1} each. A predetermined amount of EDA cross-linker was added to the BPPO solution. After stirring for 12 h, the two solutions were mixed. The mixture was cast onto a glass Petri dish and cured at 80 °C for 48 h and then at 100 °C for 2 h in a vacuum. The resultant membrane was acidified in 1 M HCl for 24 h, washed several times with distilled water, and air-dried.

The optimal SPPO to BPPO ratio, which is critical for the balance between various membrane properties such as dimensional swelling and proton conductivity, was determined first. Consequently, all the membranes in this study were prepared with this SPPO/BPPO ratio and variable EDA contents. These membranes are designated as EDA-5/1/x, where 5/1/x is the mole ratio of the functional groups ($-SO_3H/-CH_2Br/-NH_2$) used in the preparation. For example, EDA-5/1/0.15 is the membrane prepared from SPPO, BPPO, and EDA in the functional group mole ratio of 5:1:0.15. A membrane without the EDA cross-linker, EDA-5/1/0, was also prepared as the control.

2.3. Characterization. Transmission electron microscopy (TEM) images were obtained from a JEOL JEM-2010 microscope operating at 200 kV accelerating voltage. The membrane samples for TEM examination were first treated with a saturated solution of $Pb(NO_3)_2$ for 24 h to enhance the imaging contrast between ionic and nonionic domains. The treated samples, after rinsing with distilled water and drying in a vacuum, were encapsulated in an epoxy embedding medium (Sigma-Aldrich) and sectioned to 50 nm slices by a Leica ultramicrotome. The slices were then placed on a 100 mesh copper grid for TEM analysis. The thermal properties of the membranes were evaluated by differential scanning calorimetry on a METTLER TOLEDO DSC 822e in N_2 atmosphere. The membrane samples were heated from 25 to 270 °C at a rate of 10 °C min^{-1}. Dynamic mechanical analysis (DMA) of the membranes was performed on a TA Instruments DMA 2980. The analysis was carried out in air from 50 to 270 °C at 1 Hz frequency. Solid state ^{13}C NMR measurements were performed on a Bruker DRX-400 MHz NMR spectrometer operating at 100 MHz. X-ray photoelectron spectra (XPS) were collected from a Kratos Axis Ultra DLD spectrometer. All binding energies were referenced to the C1s hydrocarbon peak at 284.6 eV.

The water uptake (WU) by a membrane was determined by the difference in weights between dry (W_{dry}, g) and water-saturated states (W_{wet}, g). Water uptake was calculated as the wt % of the dry sample, i.e., WU = $((W_{wet} - W_{dry})/W_{dry}) \times 100\%$. The dimensional changes of a membrane were estimated by equilibrating a strip of sample in water at a prescribed temperature for 24 h, and then measuring the changes in length: $\Delta l = ((l_w - l_d)/l_d) \times 100\%$ (where l_w and l_d are the lengths of the wet and dry membranes, respectively). The ion exchange capacity (IEC) of a membrane was determined by acid−base titration. First, a membrane in its native H^+ form was equilibrated in 1.0 M NaCl for 24 h to fully exchange the protons with sodium cations. The acidity in the NaCl solution was then titrated with 0.01 M NaOH. IEC (mmol g^{-1}) was calculated as the moles of exchangeable protons per gram of the dry weight. Methanol permeability measurements were carried out using a two-compartment diffusion cell.[22] One of the compartments was filled with 2 M methanol solution, and the other with deionized water. A membrane fully hydrated with deionized water was inserted between the two compartments. The increase in methanol concentration in the water compartment with time was monitored by gas chromatography (Shimadzu GC2010 with flame ionization detector). Methanol permeability (P, cm^2 s^{-1}) was calculated from the slope of the $C_B(t)$ vs $t - t_0$ plot by the relation $C_B(t) = (A/V_B)(P/L)C_A(t - t_0)$, where C_A is the initial methanol concentration, $C_B(t)$ is the methanol concentration in the water compartment at time t, V_B is the volume of deionized water in the water compartment, L is

dx.doi.org/10.1021/jp2081353 | J. Phys. Chem. B 2012, 116, 6416−6424

the membrane thickness, and A is the effective diffusional area. Membrane proton conductivity was determined by the standard four-point probe technique. Impedance measurements in the frequency range 1 MHz to 50 Hz were taken by an Autolab PGSTAT 30 (Eco Chemie, Netherlands) potentiostat/galvanostat equipped with a FRA2 module (Frequency Response Analysis). The membrane resistance (R, Ω) was obtained from impedance measurements by an established procedure.[23] Proton conductivity (σ, S cm^{-1}) was then calculated from the equation $\sigma = L/RWd$, where L is the distance between the potential-sensing electrodes and W and d are the width and thickness of the sample, respectively.

2.4. Fabrication of Membrane Electrode Assembly (MEA) and DMFC Testing. Membrane electrode assemblies (MEAs) were prepared by the hot-pressing technique using the following electrodes from Alfa Aesar: unsupported Pt:Ru alloy (1:1) anode with 3.0 mg cm^{-2} total metal loading and unsupported Pt cathode with 2.0 mg cm^{-2} total metal loading. Nafion solution was used as the binder on both electrodes, and the active cell area was 5 cm^2. A wet sample membrane (or the reference Nafion 117 membrane) was placed between two commercial electrodes and hot-pressed at 125 °C and 60 kg cm^{-2} for 3 min. The resultant MEA was stored in a tightly sealed container. DMFC measurements were performed on a single-stack micro DMFC supplied by Fuel Cell Technologies Inc. A feed of 2.0 M methanol aqueous solution was delivered to the anode compartment at 5 cc min^{-1} through a micropump. Dry oxygen was fed to the cathode compartment at 50 cc min^{-1}. DMFC performance was evaluated at 50 °C. As part of the cell conditioning, all cells were rested in the open circuit condition for 30 min before any measurement was taken.

3. RESULTS AND DISCUSSION

3.1. The Formation of Ion-Pair-Reinforced SPPO/BPPO/EDA SIPN Structure. Scheme 1 illustrates the main chemistry in the preparation of the SPPO/BPPO/EDA SIPN membranes where linear SPPO as the proton source was immobilized in a cross-linked BPPO/EDA network via one-pot thermal cross-linking. Since SPPO and BPPO are derived from the same PPO parent, good blending compatibility between SPPO and BPPO was assured. A covalently cross-linked BPPO network formed by the nucleophilic substitution reaction between EDA molecules and the bromomethyl groups of BPPO established the basic membrane mechanical framework. The progressive alkylation of EDA by the bromomethyl groups formed secondary and tertiary amines in varying quantities, depending on the $-NH_2$ to $-CH_2Br$ ratio used. The quaternization of amine was however not observed under the experimental conditions (*vida infra*). Ion pairs (protonated amine-sulfonate anion) were formed by the acid−base reaction between the secondary/tertiary amines and the sulfonic acid groups of SPPO (Scheme 1), which strengthened the attachment of SPPO to the BPPO/EDA network. The direct protonation of EDA by the sulfonic acid groups of SPPO[3,7] was also likely to occur during the mixing of SPPO and BPPO solutions initially.

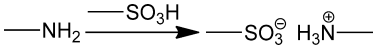

However, this acid−base reaction was soon superseded by the above-mentioned nucleophilic substitution reactions especially during curing of the membrane (*vida infra*).

The presence of different amine and ammonium moieties in the membranes was confirmed by ^{13}C solid-state NMR spectroscopy. Figure 1a and b show the ^{13}C NMR spectra of BPPO and an EDA-5/1/0.75 membrane, respectively. The six primary peaks (C_1−C_6) from 113 to 154 ppm could be assigned to the carbon atoms of the phenyl ring.[24] The peaks at around 16 and 28 ppm are characteristic of the aliphatic carbon in the methyl ($-CH_3$) and bromomethyl groups, respectively.[25] Figure 1b shows that amination of the bromomethyl group gave rise to new peaks at 37 and 49 ppm (C_7−C_8). The chemical shifts are typical of the decrease in electron density when aliphatic carbons are in close vicinity of secondary and tertiary amines, respectively.[26] This is an indirect indication that the EDA $-NH_2$ groups had reacted with the BPPO $-CH_2Br$ groups to form secondary and tertiary amine moieties. The

Scheme 1. Preparation of SIPN Membranes

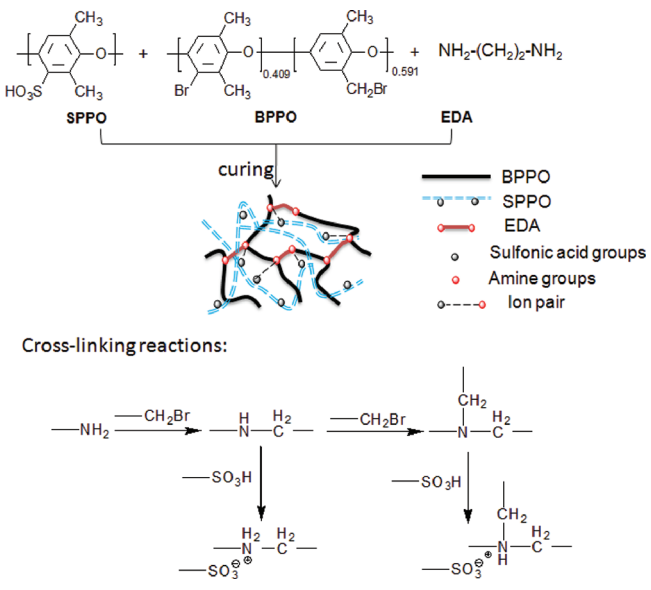

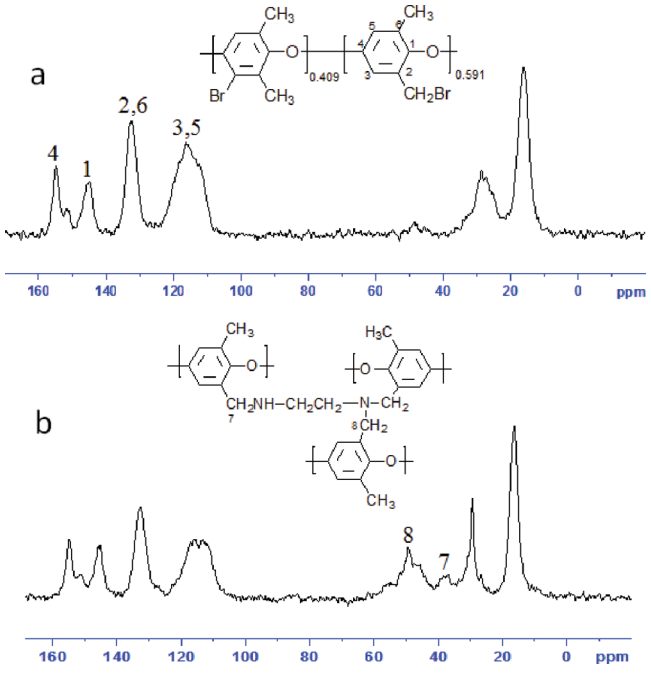

Figure 1. ^{13}C NMR spectra of BPPO and EDA-5/1/0.75 membrane.

dx.doi.org/10.1021/jp2081353 | J. Phys. Chem. B 2012, 116, 6416−6424

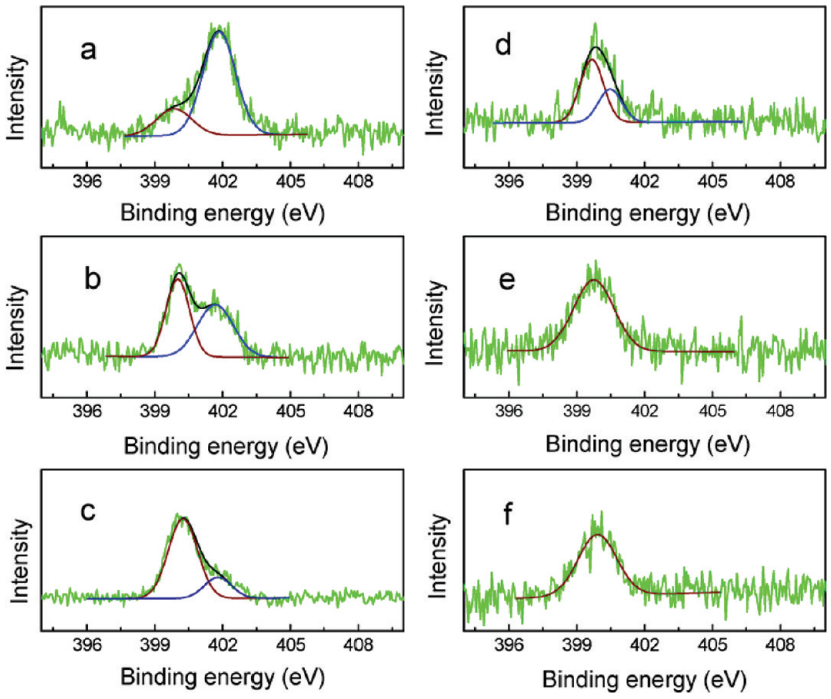

Figure 2. XPS spectra of SIPN membranes: (a) EDA-5/1/0.15, (b) EDA-5/1/0.45, (c) EDA-5/1/0.75, (d) EDA-5/1/0.15 after KOH treatment, (e) EDA-5/1/0.45 after KOH treatment, (f) EDA-5/1/0.75 after KOH treatment.

amine and ammonium moieties (protonated amines) in the SIPN membranes were also characterized by XPS (Figure 2). There were two N1s peaks centering at about 399.9 and 401.8 eV for all SIPN membranes, which could be assigned to secondary (or tertiary) amines and positively charged N^+ species, respectively.[27] The N^+ species in the XPS spectra could exist in two forms: as protonated amines (i.e., $-NH_3^+$, $-RNH_2^+$, and $-R_2NH^+$) or quaternary ammonium ($-R_3N^+$). However, they could be differentiated by treating the SIPN membranes in 2 M KOH aqueous solution for 2 days and XPS re-examination. After the base treatment, protonated amine groups would be converted back to uncharged amines (i.e., $-NH_2$, $-R_2N$, and $-RNH$), whereas $-R_3N^+$ groups would become $-R_3N^+OH^-$. The XPS spectra of the KOH treated membranes (Figure 2d–f) did not show any N^+ peak, thereby ruling out the existence of quaternary ammonium groups $-R_3N^+OH^-$. Quaternization did not occur mostly due to steric hindrance. It should also be noted that no primary amine peak was identifiable in Figure 2d–f. Hence, the initial acid–base reaction between EDA and SPPO was replaced by subsequent substitution reactions between $-CH_2Br$ and EDA, which obliterated the existence of primary amines. This could be attributed to the presence of the $-CH_2Br$ group: CH_2 in the CH_2Br group is a reactive electrophile which could weaken the stability of the $-SO_3^-\cdots{}^+NH_3-$ interaction to shift the equilibrium in the acid–base reaction toward ion pair dissociation. The elevated temperature used in curing could also improve the kinetics of the benzyl bromide attack on $-NH_2$ to form secondary or tertiary amines by nucleophilic substitution.

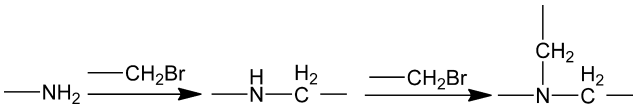

For membranes formed with a low EDA content, such as EDA-5/1/0.15, the peak intensity at 401.8 eV was significantly stronger than that at 399.8 eV (Figure 2a), suggesting that most of the amine groups were protonated and formed ion pairs with the sulfonic acid groups. With the increase in the EDA content (the EDA-5/1/0.45 and EDA-5/1/0.75 membranes), the prominence of the N1s peak at 401.8 eV diminished (Figure 2b and c). The decreasing proportion of positively charged N^+ species suggests the increase in steric hindrance when EDA cross-linking became more pervasive. Fewer $-SO_3H$ groups were sufficiently close to the amine groups to form ion pairs. The two N1s peaks of the EDA-5/1/0.15 membrane at 399.8 and 400.4 eV are characteristic of secondary and tertiary amines, respectively. The EDA-5/1/0.45 and EDA-5/1/0.75 membranes, on the other hand, showed only secondary amine peaks (Figure 2e and f). Hence, tertiary amines were not formed when the $-NH_2$ groups became abundant. This is because $-NH_2$ groups could only cross-link with proximal $-CH_2Br$ groups. An increase in the concentration of the $-NH_2$ groups depleted the $-CH_2Br$ groups locally. The likelihood of generating tertiary amines (which require a larger number of proximal $-CH_2Br$ groups) relative to the secondary amines therefore decreased as a result.

The distribution of sulfonic acid clusters in the membrane matrix was inferred from TEM images of membrane cross sections (Figure 3). The dark spots in the TEM images were sulfonic acid clusters stained by Pb^{2+} ions (as lead sulfonate) to improve the image contrast.[28] Figure 3a shows the cross section of the control sample of un-cross-linked EDA-5/1/0 membrane. The Pb^{2+} stained sulfonic acid cluster spots were highly clustered and ununiformly distributed. This is probably an indication of significant hydrophobic rejection of the $-SO_3H$ groups by the PPO backbone and the $-CH_2Br$ groups to form inverted micelle-like structures with sulfonic acid groups on the inside and hydrophobic segments (BPPO and unsulfonated PPO) on the outside.[29,30] The dispersion of sulfonic acid

dx.doi.org/10.1021/jp2081353 | J. Phys. Chem. B 2012, 116, 6416–6424

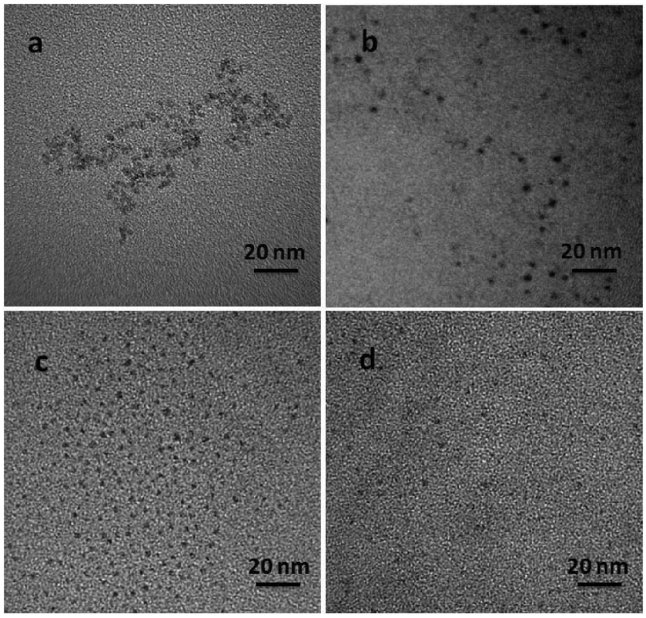

Figure 3. TEM images of the cross sections of (a) EDA-5/1/0, (b) EDA-5/1/0.15, (c) EDA-5/1/0.45, and (d) EDA-5/1/0.75.

clusters was significantly improved by EDA cross-linking, since all SIPN polymers showed more homogeneity of the lead sulfonate spots (Figure 3b–d). This could be attributed to following two contributions from cross-linking. First, the amine moieties at the cross-linking points are hydrophilic and as such decreased the hydrophobic rejection effect to result in a less pronounced microscopic phase separation. At the same time, ion pair formation between the amine moieties and the sulfonic acid groups increased the infiltration of SPPO into the cross-linked BPPO network. The more uniform distribution of the sulfonic acid clusters was also confirmed by small-angle X-ray scattering (SAXS) measurements (Supporting Information, Figure S1). The absence of a visible peak in the small angle region (0–0.35 $Å^{-1}$ in scattering vector (q)) suggests a high dispersion of small sulfonic acid clusters in the polymer matrix.[31] The uniform distribution of sulfonic acid clusters made it more likely to form a connected network of hydrophilic domains upon water absorption to facilitate proton transport. Among the SIPN membranes, the one formed with a moderate EDA content (EDA-5/1/0.45) had the most uniform distribution of the sulfonic acid clusters. It is theorized that low EDA content (e.g., EDA-5/1/0.15) formed predominantly tertiary amine cross-linking points, and high EDA content (EDA-5/1/0.75) formed a dense and excessively cross-linked network. Both were significant steric barriers to the uniform distribution of the sulfonated acid clusters. Hence, an intermediate EDA content was more likely to achieve a balanced outcome for effective proton conduction through the membrane.

3.2. Thermal and Mechanical Properties. The results from ^{13}C NMR, XPS, and TEM all hinted at the formation of an ion-pair-reinforced interlocked SIPN structure. DSC and DMA measurements were subsequently used to provide further experimental evidence.

For DSC measurements, the membrane samples were subjected to two consecutive scans: an initial conditioning scan from 25 to 150 °C followed immediately by the measurement scan from 25 to 270 °C. Figure 4 shows the

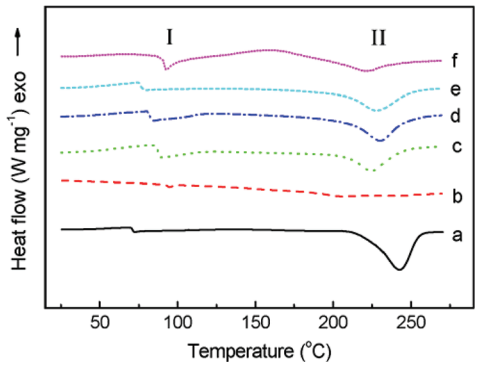

Figure 4. DSC curves of SPPO (a), BPPO (b), EDA-5/1/0 (c), EDA-5/1/0.15 (d), EDA-5/1/0.45 (e), and EDA-5/1/0.75 (f).

second-scan DSC thermograms of SPPO, BPPO, and four SIPN membranes. Two endothermic transitions could be detected between 50 and 250 °C in the DSC thermograms of SPPO and SIPN membranes. The first endothermic peak (I) at lower temperatures has been observed for other ionomers (e.g., Nafion), although its assignment is still under debate. Page et al.,[32] for example, considered this peak as the melting of small imperfect polymer crystals. Goddard et al.,[33] on the other hand, attributed this endothermic peak to enthalpy associated with water vaporization and water leaving the coordination environment of ions. Since the second scan in this study was run right after the first one, volatile solvent and water should all have been eliminated after the heating in the first scan. Consequently, we are more inclined to attribute the first endothermic peak to the movement of short, unsulfonated PPO chain segments of SPPO. The sulfonation process placed sulfonic acid groups on the PPO chains at nearly regular intervals and increased the interchain distance between unsulfonated segments. The relaxation of the spatial constraint on the segmental motion of unsulfonated segments is shown by a glass transition temperature (T_g) which is well below that of pristine PPO (211 °C). Figure 4 also shows a fairly broad second endothermic peak (II) around 243 °C for SPPO indicative of the clustering of the sulfonic acid groups due to hydrogen bonding and dipole–dipole interactions.[34] These intra- and intermolecular forces hindered the rotation of the sulfonated phenyl rings relative to the unsulfonated segments.

Different from SPPO, BPPO showed a very gentle glass transition at around 175 °C. This is because the bulky bromomethyl group increased the polymer free volume, allowing the segments to move more freely. Less energy was therefore required for glass transition.

For the EDA-5/1/0 membrane, the second endothermic peak was shifted to a lower temperature than SPPO. This could be caused by the partitioning effect of BPPO which disrupted the clustering of the sulfonic acid groups and weakened the interactions in the latter responsible for chain rotation impediment. The shape of the second endothermic peak (II) and the peak temperatures of the three SIPN membranes also display an interesting trend: with a $-CH_2Br/-NH_2$ ratio of 1/0.15, the peak temperature was about 7 °C higher than that of EDA-5/1/0, indicating the constriction effect imposed by cross-linking and protonated amine–sulfonate ion pairs. When the ratio was increased to 1/0.45, there was no increase in the peak temperature but peak broadening was observed. Further increases of the ratio to 1/0.75 resulted in a lower temperature and a broader peak. Peak broadening is an indication of a more

dx.doi.org/10.1021/jp2081353 | J. Phys. Chem. B 2012, 116, 6416–6424

continuous distribution of energy barriers against the thermal motion of sulfonic acid groups. The multitude of interactions between sulfonic acid groups—hydrogen bonding, dipole–dipole interactions, and ion pair formation—was likely the reason. The changes in the peak temperature of the second endothermic peak (II) were also mirrored by the DMA measurements. In Figure 5, the tan δ–T curves show three

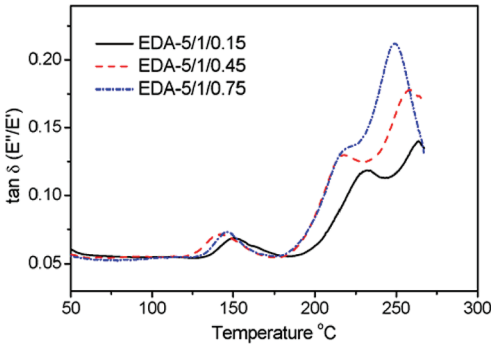

Figure 5. Temperature dependence of tan δ of SIPN membranes.

types of relaxations in the SIPN membranes: a weak β relaxation centering about 140 °C and two intense peaks above 200 °C. The weak β relaxation could be attributed to the chain motion of short unsulfonated PPO segments.[35] The two intense peaks correspond well with the broad second endothermic peak (II) in the DSC thermograms. The lower temperature peak could be related to interactions such as hydrogen bonding, dipole–dipole interactions between the sulfonic acid groups, and ion pairs, while the higher temperature peak related more to the relaxation of the entire SIPN structure. It was found that, as the EDA content increased from 0.15 to 0.75, both peaks were shifted to lower temperatures. This could be caused by the weaker interactions between the ion pairs at high EDA contents, when strongly basic tertiary amines were progressively replaced by less basic secondary amines. In addition, a higher extent of EDA cross-linking also interrupted the clustering of sulfonic acid groups and confined the latter to several nanoscale domains. The interaction between the sulfonic acid groups decreased as a result. This result corroborated the previous inference that a high cross-linking degree would impede the clustering of sulfonic acid groups.

3.3. Evaluation of the SPPO/BPPO/EDA SIPN Membranes for DMFC Applications. The variations in IEC and proton conductivity as functions of the EDA content are shown in Figure 6. The good agreement between the measured IEC of

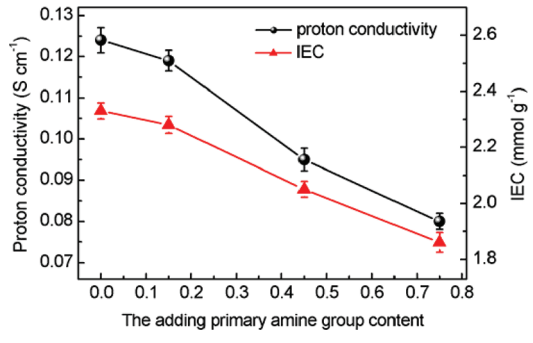

Figure 6. The IEC and proton conductivity of SIPN membranes.

0.95 mmol g^{-1} for Nafion 117 and the literature value[36] validated the measurement method. As expected, the IEC values correlated negatively with the EDA content of the SIPN membranes. This could be understood from the depletion of free sulfonic acid groups due to the formation of protonated amine–sulfonate ion pairs. Proton dissociation from protonated secondary/tertiary amines was a more difficult affair. The protonated amine moiety contents of EDA-5/1/0 and three SIPN membranes were measured (Table 1). The values were 0.06, 0.13, and 0.28 mmol g^{-1} for EDA-5/1/0.15, EDA-5/1/0.45, and EDA-5/1/0.75, respectively. The increase in the number of protonated amine–sulfonate ion pairs and cross-linking degree caused a decrease in proton conductivity from EDA-5/1/0.15 to EDA-5/1/0.75. It should however be mentioned the decrease in proton conductivity was more moderate at high ion pair contents. Specifically, the proton conductivity decrease from EDA-5/1/0.45 to EDA-5/1/0.75 (15.7%) was lower than the proton conductivity decrease from EDA-5/1/0.15 to EDA-5/1/0.45 (20.2%), even though the percentage increase in ion pairs in these two cases was about the same. This could be attributed to the compensation effects of the hydrophilic cross-links which negated partially the proton conductivity decrease caused by the depletion of free sulfonic acid groups. These values also represent an improvement over our previous design of ionically cross-linked PPO-based membranes,[22] indicating the more effective proton conduction in a SIPN structure than in simple ionic cross-linking. Compared with a proton conductivity of 9.0×10^{-2} S cm^{-1} for Nafion 117, the proton conductivities of SIPN membranes from 11.9×10^{-2} to 8.0×10^{-2} S cm^{-1} are definitely adequate for fuel cell applications.

Figure 7 shows the water uptake by the SIPN membranes. For comparison, the water uptake of the non-cross-linked EDA-5/1/0 membrane was also measured (72.0 wt %). The water uptake by the SIPN membranes was noticeably lower than that of the EDA-5/1/0 membrane, and decreased with the increase in the EDA content from 58.8 wt % (the EDA-5/1/0.15 membrane) to 35.8 wt % (the EDA-5/1/0.75 membrane). This was clearly a consequence of cross-linking. Increase in the EDA content increased the number of cross-links in the membrane matrix. The expansion of polymer chains under hydration conditions became more restricted. The reduction in water accommodation capability translated into a decreased water uptake. The trend in dimensional swelling (Figure 8) mirrored that of water uptake: the SIPN membranes underwent smaller dimensional changes than the un-cross-linked EDA-5/1/0 membrane, and swelling decreased with the increase in EDA content. The dimensional changes of 13.8% at 25 °C and 22.8% at 80 °C for EDA-5/1/0.75 were lower than the corresponding values of EDA-5/1/0 (28.0% at 25 °C and 42.4% at 80 °C), indicating the positive contribution of a cross-linked network on suppressing membrane swelling.

The methanol permeability of the SIPN membranes was then measured to evaluate the suitability of these membranes for DMFC operations. The methanol permeability of the SIPN membranes is shown in Figure 9. The methanol permeability of Nafion 117 measured under the same experimental conditions was 2.01×10^{-6} cm^2 s^{-1}, which is consistent with the published value.[37] The pristine EDA-5/1/0 membrane without any cross-linking was 41% lower than that of Nafion 117. Methanol permeability decreased further from 1.40×10^{-6} cm^2 s^{-1} (EDA-5/1/0) to ~3.31×10^{-7} cm^2 s^{-1} (EDA-5/1/0.75) after cross-linking. Hence, an order of magnitude improvement over

dx.doi.org/10.1021/jp2081353 | J. Phys. Chem. B 2012, 116, 6416–6424

Table 1. Results of IEC, Oxidation, and Hydrolytic Stability of SIPN Membranes

			oxidative stability	hydrolytic stability	
				proton conductivity (S cm^{-1})	
membrane	IEC (mmol g^{-1})	protonated amine content[a] (mmol g^{-1})	weight loss in Fenton's test (%)	before	after
EDA-5/1/0	2.33	0	2.1	0.124	0.123
EDA-5/1/0.15	2.28	0.06	1.8	0.119	0.113
EDA-5/1/0.45	2.05	0.13	1.4	0.095	0.089
EDA-5/1/0.75	1.86	0.28	1.3	0.080	0.079
Nafion 117	0.95		0.5	0.090	0.087

[a]The SIPN membranes were neutralized by KOH solution first and then equilibrated by HCl solution. The protonated amine content was then determined from the following equation: protonated amine content = (no. of moles of HCl equilibrated with membrane)/(dry mass of membrane, m_{dry}) − IEC.

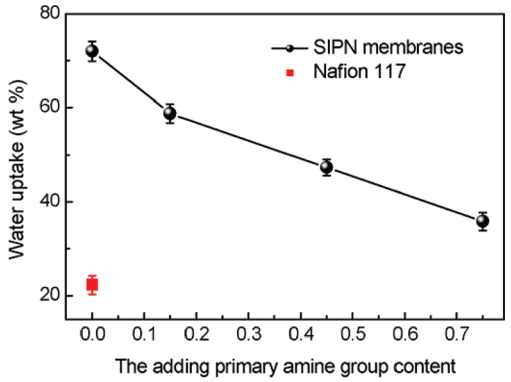

Figure 7. Water uptake measurements.

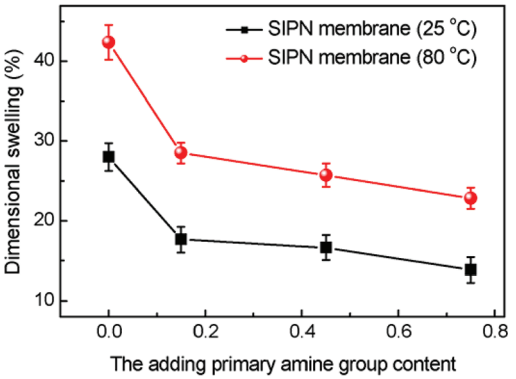

Figure 8. Dimensional swelling in SIPN membranes.

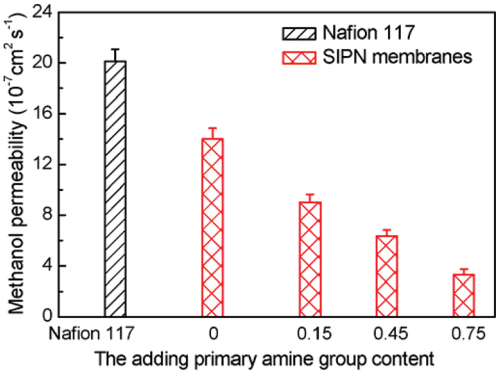

Figure 9. Methanol permeability of Nafion 117 and SIPN membranes.

Nafion 117 was possible. Especially for EDA-5/1/0.75, methanol permeability was about 6 times lower than Nafion 117. The low methanol permeability of cross-linked SIPN membranes could be attributed to the more compact structure of a cross-linked network which is a hindrance to the transport of methanol molecules.

Proton conductivity and methanol permeability are two important transport properties of a PEM. It is desirable to have high proton conductivity together with low methanol crossover. A composite indicator may be used to evaluate the selectivity in proton and methanol transport. Selectivity has been defined as the ratio of fluxes in some published papers.[38] However, a selectivity defined as such is susceptive to external factors such as the operating conditions. Hence, we prefer the use of selectivity which is based on membrane intrinsic properties. The ratio of proton conductivity to methanol permeability, known in the fuel cell community as the "characteristic factor", was therefore the composite indicator adopted for this study.[39,40] Figure 10 shows the characteristic factor of the

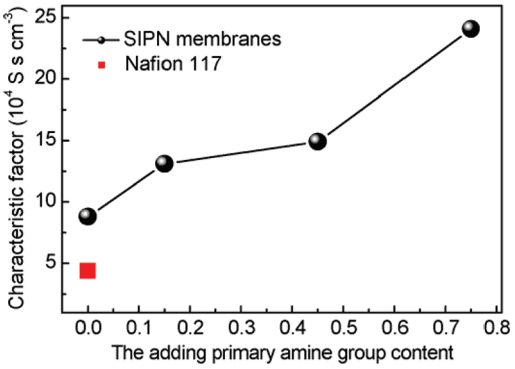

Figure 10. Characteristic factor of Nafion 117 and SIPN membranes.

SIPN membranes as a function of the EDA content. It is apparent that the characteristic factors of the SIPN membranes were all higher than that of Nafion 117 and increased with increasing EDA content. Among the SIPN membranes, EDA-5/1/0.75 had the highest characteristic factor of 24.1 × 10^4 S s cm^{-3} which nearly doubled the value of EDA-5/1/0.

The oxidative and hydrolytic stability of the membranes were also measured and summarized in Table 1. Here, the oxidative stability of the membranes was evaluated by the Fenton test (chemical stability in 3 wt % H_2O_2 aqueous solution containing 3 ppm $FeCl_2{\cdot}4H_2O$) at 80 °C.[41] All membranes retained more than 97% of the initial weights after 1 h in the Fenton solution. Compared to a weight loss of 2.1% for the EDA-5/1/0 membrane, the SIPN membranes fared much better (with weight loss of 1.8, 1.4, and 1.3% for EDA-5/1/0.15, EDA-5/1/

dx.doi.org/10.1021/jp2081353 | J. Phys. Chem. B 2012, 116, 6416−6424

0.45, and EDA-5/1/0.75, respectively), showing improved stability after cross-linking. The hydrolytic stability of the membranes was investigated by comparing the proton conductivities before and after equilibrium in 80 °C water for 2 weeks. All membranes showed negligible changes in conductivity.

The EDA-5/1/0.75 membrane, with a high proton conductivity (8.0×10^{-2} S cm^{-1}), acceptable water uptake and dimensional swelling, and low methanol permeability (3.31×10^{-7} cm^2 s^{-1}), appears to have the best balance for DMFC applications, and was therefore chosen for single-stack fuel cell tests. The performance of the cell is shown in Figure 11

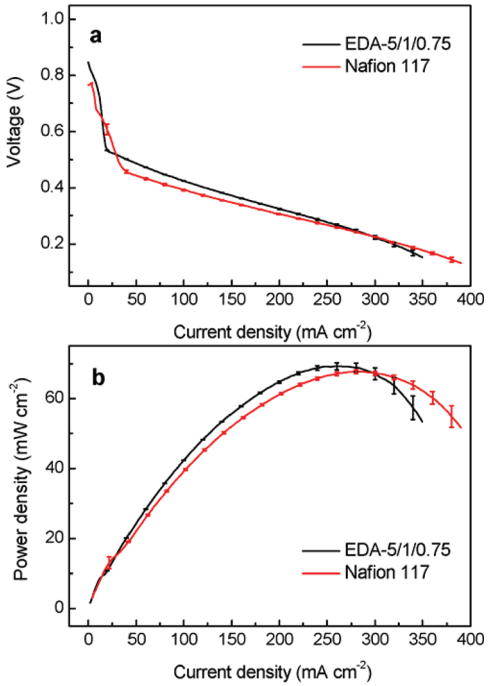

Figure 11. Single-stack DMFC tests of Nafion 117 MEA and an EDA-5/1/0.75 MEA at 50 °C with 2.0 M methanol: (a) voltage−current density plot; (b) power density−current density plot.

alongside that of a commercial Nafion 117 membrane fuel cell. The MEA fabricated from the EDA-5/1/0.75 membrane had a slightly better performance than the Nafion 117 MEA. The maximum power density derivable from the EDA-5/1/0.75 MEA was about 69.3 mW cm^{-2} at 262 mA cm^{-2}, while the Nafion 117 MEA delivered 67.7 mW cm^{-2} at 284 mA cm^{-2}. The open circuit voltage (OCV) was also higher for the EDA-5/1/0.75 (0.85 V) MEA than the Nafion 117 MEA (0.76 V). The better performance of the EDA-5/1/0.75 MEA suggested that the SIPN membranes have great potential for DMFC applications. However, the fabrication technique has to be optimized for the SIPNs in order to fully utilize the materials advantage of the latter.

4. CONCLUSIONS

In this study, new ion-pair-reinforced SIPN membranes were prepared by thermally cross-linking EDA and BPPO in the presence of linear SPPO. The SIPN structure was deduced from ^{13}C NMR, XPS, and TEM and corroborated by DSC and DMA measurements. During the in situ cross-linking process, different amine moieties (secondary, tertiary, and protonated amines) were formed in quantities that depended on the amount of EDA used in the preparation. Subsequent ion pair formation between the generated amine moieties and the sulfonic acid groups of SPPO enhanced the immobilization of SPPO in the BPPO network and the uniformity of sulfonic acid cluster distribution in the membrane. It was found that the accessibility of sulfonic acid clusters and hence the proton transport and mechanical properties of the membranes were dependent on the EDA cross-linking degree, with a moderate cross-linking degree delivering the most desirable outcome. The ion-pair-reinforced SIPN membranes displayed good proton conductivity, good dimensional stability up to 80 °C, and low methanol permeability. The greater single cell performance of EDA-5/1/0.75 MEA compared to Nafion 117 MEA also demonstrated the potential of SIPN membranes for DMFC applications.

■ ASSOCIATED CONTENT

Supporting Information

Small angle X-ray scattering (SAXS) spectra of the as-prepared membranes. This material is available free of charge via the Internet at http://pubs.acs.org.

■ AUTHOR INFORMATION

Corresponding Author

*Phone: +65-6516-5029 (L.H.); +65-6874-2899 (J.Y.L.). Fax: +65-6779-1936 (L.H.); +65-6779-1936 (J.Y.L.). E-mail: chehongl@nus.edu.sg (L.H.); cheleejy@nus.edu.sg (J.Y.L.).

Notes

The authors declare no competing financial interest.

■ ACKNOWLEDGMENTS

C.F. acknowledges the research scholarship support from the National University of Singapore Graduate School for Integrative Science and Engineering (NGS).

■ REFERENCES

(1) Hickner, M. A.; Pivovar, B. S. *Fuel Cells* **2005**, *5*, 213−229.
(2) Chang, H. Y.; Lin, C. W. *J. Membr. Sci.* **2003**, *218*, 295−306.
(3) Kerres, J. A. *Fuel Cells* **2005**, *5*, 230−247.
(4) Kerres, J. A. *J. Membr. Sci.* **2001**, *185*, 3−27.
(5) Ye, Y. S.; Yen, Y. C.; Cheng, C. C.; Chen, W. Y.; Tsai, L. T.; Chang, F. C. *Polymer* **2009**, *50*, 3196−3203.
(6) Xue, Y.; Fu, R.; Wu, C.; Lee, J. Y.; Xu, T. *J. Membr. Sci.* **2010**, *350*, 148−153.
(7) Wu, D.; Xu, T. W.; Wu, L.; Wu, Y. H. *J. Power Sources* **2009**, *186*, 286−292.
(8) Kerres, J.; Zhang, W.; Jorissen, L.; Gogel, V. *J. New Mater. Electrochem. Syst.* **2002**, *5*, 323−323.
(9) Kerres, J. *Fuel Cells* **2006**, *6*, 251−260.
(10) Kerres, J.; Hein, M.; Zhang, W.; Graf, S.; Nicoloso, N. *J. New Mater. Electrochem. Syst.* **2003**, *6*, 223−229.
(11) Rohman, G.; Grande, D.; Laupretre, F.; Boileau, S.; Guerin, P. *Macromolecules* **2005**, *38*, 7274−7285.
(12) Kwon, Y. H.; Kim, S. C.; Lee, S. Y. *Macromolecules* **2009**, *42*, 5244−5250.
(13) Lin, C. W.; Huang, Y. F.; Kannan, A. M. *J. Power Sources* **2007**, *171*, 340−347.
(14) Huang, Y. F.; Chuang, L. C.; Kannan, A. M.; Lin, C. W. *J. Power Sources* **2009**, *186*, 22−28.
(15) Tsai, C.-E.; Lin, C.-W.; Hwang, B.-J. *J. Power Sources* **2010**, *195*, 2166−2173.
(16) Gitsov, I.; Zhu, C. *J. Am. Chem. Soc.* **2003**, *125*, 11228−11234.
(17) Lumelsky, Y.; Zoldan, J.; Levenberg, S.; Silverstein, M. S. *Macromolecules* **2008**, *41*, 1469−1474.

(18) Davion, B.; Vancaeyzeele, C.; Fichet, O.; Teyssie, D. *Polymer* **2010**, *51*, 5323−5331.
(19) Xu, T. W.; Wu, D.; Wu, L. *Prog. Polym. Sci.* **2008**, *33*, 894−915.
(20) Huang, R. Y. M.; Kim, J. J. *J. Appl. Polym. Sci.* **1984**, *29*, 4017−4027.
(21) Kruczek, B.; Matsuura, T. *J. Membr. Sci.* **1998**, *146*, 263−275.
(22) Fu, R. Q.; Julius, D.; Hong, L.; Lee, J. Y. *J. Membr. Sci.* **2008**, *322*, 331−338.
(23) Sone, Y.; Ekdunge, P.; Simonsson, D. *J. Electrochem. Soc.* **1996**, *143*, 1254−1259.
(24) Bonfanti, C.; Lanzini, L.; Roggero, A.; Sisto, R. *J. Polym. Sci., Part A: Polym. Chem.* **1994**, *32*, 1361−1369.
(25) White, D. M.; Nye, S. A. *Macromolecules* **1990**, *23*, 1318−1329.
(26) Sarneski, J. E.; Surprenant, H. L.; Molen, F. K.; Reilley, C. N. *Anal. Chem.* **1975**, *47*, 2116−2124.
(27) Cheng, Z. P.; Zhu, X. L.; Shi, Z. L.; Neoh, K. G.; Kang, E. T. *Surf. Rev. Lett.* **2006**, *13*, 313−318.
(28) Lee, M.; Park, J. K.; Lee, H. S.; Lane, O.; Moore, R. B.; McGrath, J. E.; Baird, D. G. *Polymer* **2009**, *50*, 6129−6138.
(29) Mauritz, K. A.; Moore, R. B. *Chem. Rev.* **2004**, *104*, 4535−4585.
(30) Schmidt-Rohr, K.; Chen, Q. *Nat. Mater.* **2008**, *7*, 75−83.
(31) Essafi, W.; Gebel, G.; Mercier, R. *Macromolecules* **2004**, *37*, 1431−1440.
(32) Page, K. A.; Cable, K. M.; Moore, R. B. *Macromolecules* **2005**, *38*, 6472−6484.
(33) Goddard, R. J.; Grady, B. P.; Cooper, S. L. *Macromolecules* **1994**, *27*, 1710−1719.
(34) Carbone, A.; Pedicini, R.; Portale, G.; Longo, A.; D'Ilario, L.; Passalacqua, E. *J. Power Sources* **2006**, *163*, 18−26.
(35) Di Noto, V.; Boaretto, N.; Negro, E.; Pace, G. *J. Power Sources* **2010**, *195*, 7734−7742.
(36) Bai, Z. W.; Houtz, M. D.; Mirau, P. A.; Dang, T. D. *Polymer* **2007**, *48*, 6598−6604.
(37) Elabd, Y. A.; Napadensky, E.; Sloan, J. M.; Crawford, D. M.; Walker, C. W. *J. Membr. Sci.* **2003**, *217*, 227−242.
(38) Pivovar, B. S.; Wang, Y. X.; Cussler, E. L. *J. Membr. Sci.* **1999**, *154*, 155−162.
(39) Nasef, M. M.; Zubir, N. A.; Ismail, A. F.; Dahlan, K. Z. M.; Saidi, H.; Khayet, M. *J. Power Sources* **2006**, *156*, 200−210.
(40) Wu, D.; Fu, R. Q.; Xu, T. W.; Wu, L.; Yang, W. H. *J. Membr. Sci.* **2008**, *310*, 522−530.
(41) Tripathi, B. P.; Chakrabarty, T.; Shahi, V. K. *J. Mater. Chem.* **2010**, *20*, 8036−8044.